Amer *et al. Beni-Suef Univ J Basic Appl Sci* (2024) 13:39
https://doi.org/10.1186/s43088-024-00498-6

Beni-Suef University Journal of Basic and Applied Sciences

RESEARCH

Open Access

Chemical composition, antioxidant, cytotoxic, antiviral, and lung-protective activities of *Salvia officinalis* L. ethanol extract herb growing in Sinai, Egypt

Asmaa A. Amer[1*], Samar H. Kassem[2] and Mohammed Abdalla Hussein[3]

Abstract

Background Pulmonary fibrosis (PF) is a respiratory ailment that causes the substitution of healthy lung tissue with scar tissue due to collagen deposition and fibroblast proliferation. The incidence of PF increased with the successive waves of Coronaviruses and other viruses affecting the lungs. Therefore, the priority is moving toward treatment with medicinal plants for their active constituents. *Salvia officinalis* L. herbal drug (sage, family; Lamiaceae) is characterized by its strong antioxidative activity. This study aims to declare the effect of using sage ethanol extract (SOEE) as a protective agent from PF through an in vivo study on mercuric chloride **(**$HgCl_2$)-induced lung fibrosis and in vitro evaluation of its anticancer, antiviral, and antioxidant activities concerning its phytoconstituents.

Results Twelve compounds were isolated and identified as apigenin, luteolin, genkwanin, quercetin, hispidulin, luteolin-7-*O*-*β*- glucopyranoside, rutin, rosmarinic acid, caffeic acid, ferulic acid chlorogenic acid, and ellagic acid. The results of antioxidants indicated that SOEE exhibited the greatest efficacy as an antioxidant agent in the 1,1-Diphenyl-2-picrylhydrazyl assay with inhibitory concentration (IC_{50}) 23.21 ± 1.17 µg/ mL followed by 1864.71 and 1793.80 µM Trolox equivalent/mg extract for ferric ion reducing antioxidant power and 3-ethylbenzothiazoline-6-sulfonic acid (ABTS), respectively. SOEE showed notable cytotoxic activity against A549. Oral administration of SOEE at 69.4 and 173.5 mg/kg.bw afforded a noteworthy protective effect against $HgCl_2$-induced pulmonary fibrosis. Also, lung superoxide dismutase (SOD), catalase (CAT), and reduced glutathione (GSH) were increased by SOEE. That was in parallel with working to reduce the malondialdehyde (MDA), necrosis factor kappa (NF-κB), interleukin-1β (IL-1β), and cyclooxygenase-2 (COX-2) levels. The lung P53, Bcl-2, Bcl-XL, AKT, and vanin-1 gene expression was upregulated in SOEE-treated rats compared to $HgCl_2$-treated rats.

Conclusion SOEE reduces acute lung injury and can be used to inhibit the proliferation and migration of lung fibrotic cells. These activities may be related to its high antioxidant activity, which could result from the phenolic constituents. The authors recommended using sage in the treatment of lung diseases to protect from lung fibrosis. Additional animal and human experiments are needed for future research.

Keywords *Salvia officinalis* L., Sage, Anti-oxidant, Antiviral, Phenolic constituents, Cytotoxicity, Lung fibrosis

*Correspondence:
Asmaa A. Amer
asmaa_3amer86@hotmail.com
Full list of author information is available at the end of the article

Graphical abstract

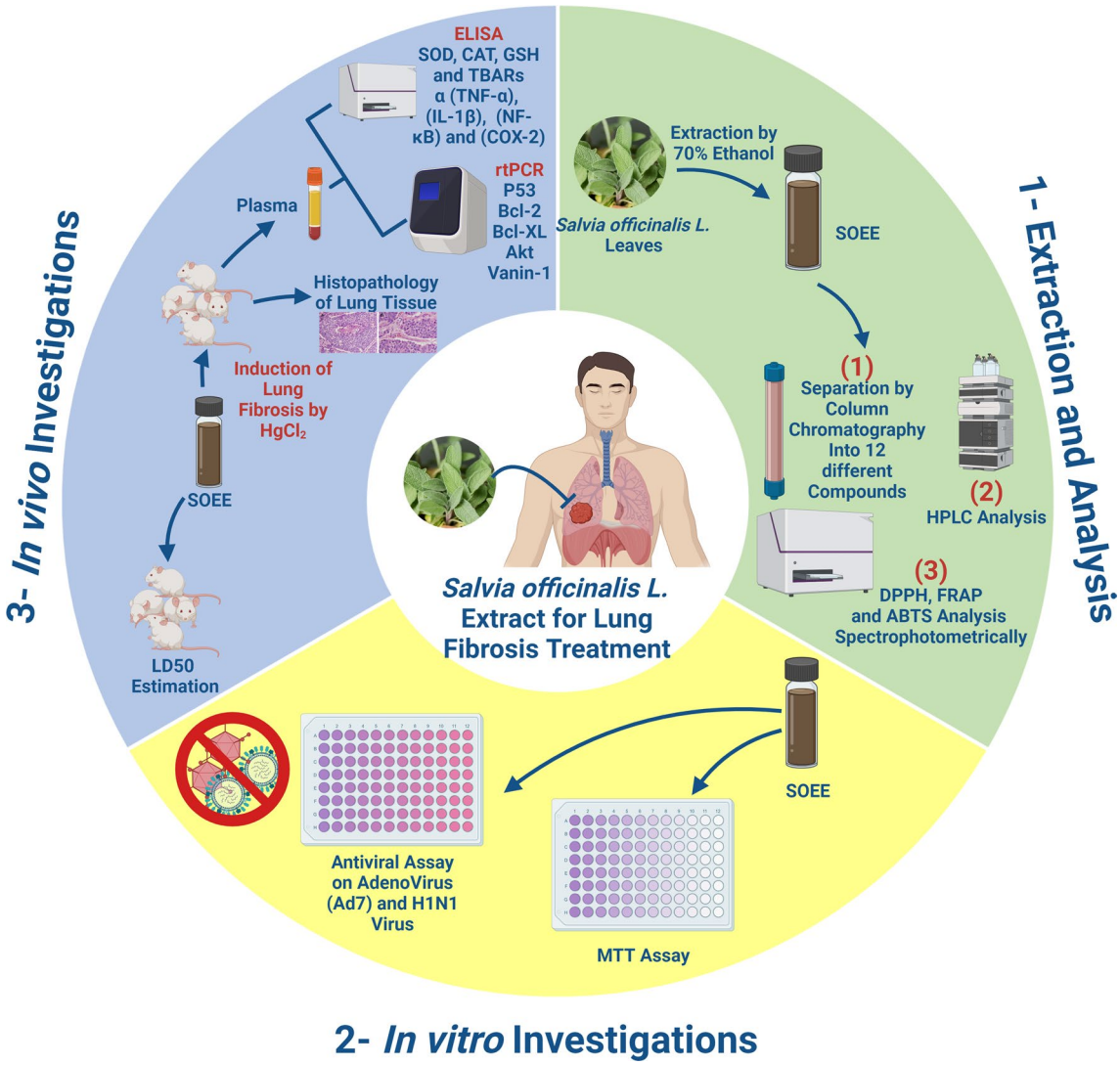

1 Background

Pulmonary fibrosis (PF) or lung fibrosis (LF) is a dangerous complication of many respiratory disorders; it is considered the end stage of heterogeneous interstitial lung diseases, injury, and inflammation [1]. LF causes an increase in the thickness of the alveolar wall and a decrease in lung functions, compliance, and capacity, which leads to failure in the respiration process [2, 3]. The occurrence of viral infections (VI) represents a risk factor for exposure to pulmonary fibrosis even after a long-term infection [4]. It can appear as a secondary lung viral infection. The relationship between LF and VI has become clearer and more widespread after the spread of severe acute respiratory syndrome (SARS) and coronavirus (COVID-19) pandemic diseases [2]. It was documented that most viruses like adenoviruses [5], influenza virus, avian influenza virus, SARS-CoV and SARS-CoV-2 [1], human T-cell leukemia virus (HTLV), hepatitis C virus (HCV) [5], human immunodeficiency virus (HIV), cytomegalovirus (CMV), Epstein–Barr virus (EBV), Middle East respiratory syndrome (MERS)-CoV, and murine γ-herpes virus 68 (MHV-68) cause long-term damage to the lung. Due to the enormous scope of COVID-19 with different waves, we expect an increase in PF that may be attributed to COVID-19 infection or other viruses that have the same symptoms and similar infections [3].

There is three-phase model in the treatment of PF which includes injury, inflammation, and repair [6].

Human adenoviruses (Ads) have numerous serotypes which cause various clinical syndromes. Notably, among the recognized serotypes, Ad type 7 (Ad7) is the most commonly associated with severe disease. This type most commonly causes mild upper respiratory tract illness and conjunctivitis, but it can also result in more severe lower respiratory tract illness, disseminated disease, and even mortality, particularly among infants and individuals with compromised immune or respiratory systems. Furthermore, Ad7 infections have been linked to central nervous system disorders and long-term respiratory complications like bronchiectasis and hyperlucent lung, also known as McLeod syndrome. WHO reported that Ad7 accounts for nearly 20% of all Ads, and there have been family clusters as well as institutional and community-wide outbreaks of Ad7 disease [7].

Human influenza subtype 1 (H1N1) influenza, also known as swine flu, is a variant of influenza A virus that causes a communicable viral disease resulting in upper and lower respiratory tract infections. The major symptoms include nasal secretions, fever, chills, reduced appetite, and, in severe cases, lower respiratory tract disease [8]. World Health Organization (WHO), 2009 [9], declared that H1N1 influenza and SARS-CoV-2 (Corona) were global pandemic diseases in 2009 and March 2020, respectively. They have the same symptoms, but Corona had the most severity [10].

The inflammation accomplished by VI resulted in a disturbance between antioxidant defense and oxidative stress [11]. SOD, CAT, and GSH enzymes are considered crucial enzymes in the enzymatic antioxidant defense system [12, 13]. SOD facilitates the conversion of superoxide radicals into H_2O_2 which is harmless through a process called dismutation [14]. Catalase is a heme protein that facilitates the reduction of hydrogen peroxide and safeguards the tissues against hazardous-harmful hydroxyl radicals [12].

GSH has a complex role in protecting against oxidative damage by acting as an antioxidant. It scavengers free radicals and also serves as a co-substrate for the detoxification of peroxide by glutathione peroxidases [15].

The Bcl-2 family proteins, which include both pro- and antiapoptotic members, play a role in the p53 apoptotic pathway [16]. The balance between these proteins, which have positive and negative regulatory functions, is crucial for determining the susceptibility to apoptosis [17]. All Bcl-2 family-associated proteins are functionally linked to mitochondria. Bcl-2, which is a representative of anti-apoptotic proteins, and Bcl-XL, which is commonly known as a pro-apoptotic factor, play roles in the later stage of programmed cell death and have contrasting activities. Cells are protected from apoptosis, which is induced by cytotoxic substances or cellular stress when there is a significant amount of Bcl-2 expression [18].

Vanin1 is an external enzyme that primarily carries out physiological tasks through the products of enzyme catalysis, which include pantothenic acid and cysteamine. The relation between Vanin1 metabolism and oxidative stress has gained significant attention in recent years [19]. Due to Vanin1's capability to impact several metabolic pathways and either worsen or alleviate pathological processes through oxidative stress, it has emerged as a crucial factor in the advancement of diseases [20].

Akt, a serine/threonine protein kinase, has been involved in suppressing cell death triggered by various stimuli such as growth factor withdrawal, cell cycle disruption, DNA damage, and loss of cell adhesion in diverse types of cells. Studies have demonstrated that organ toxicity stimulates Akt phosphorylation at Thr308 and Ser473 residues, leading to phosphorylation of the Bcl-2, which leads to the release of Bcl-XL [21].

Many rural people around the world still depend on the traditional use of herbal plants for the cure of some diseases [22–24]. In that respect, obtaining a scientific foundation for the potential application of herbal medicines in the treatment of illnesses, including viral infection, cancer, infectious disorders, and those linked to oxidative damage seems appropriate [25, 26].

Salvia officinalis L. (sage, family; Lamiaceae) is one of the most important herbal drugs widely used in folk medicine, cooking, and cosmetics [27]. The aerial parts of sage are characterized by its flavoring and seasoning properties that make them popular in the preparation of many foods [28]. The plant is common in the Middle East and Mediterranean areas [29], and nowadays, it is widely spread all over the world; Europe and North America [30]. In Egypt, it is a particular appendage in the South Sinai. Traditionally, sage has been used as an anti-inflammatory, antioxidant, antimicrobial, antidementia, and hypoglycemic drug around the world [28]. In Egypt, it is used in the treatment of upper respiratory tract disorders; asthma [31]. Several reports were traced concerning the biological activities of sage; antioxidant, anti-inflammatory, antimicrobial, and others that were attributed to its main phenolic constituents [32].

As a result of the widespread of successive waves of Coronavirus and other viruses that have similar and vigorous symptoms, causing LF and moving toward treatment with medicinal plants for their active constituents, this study aims to show the results of using SOEE as a protective agent from PF through in vivo study on $HgCl_2$-induced lung fibrosis and in vitro evaluation of its anticancer, antiviral, and antioxidant activities concerning the phytoconstituents, especially phenolics. This

study was carried out on sage growing in South Sinai, Egypt. This plant was chosen based on ethnobotanical knowledge, evidence of continued widespread use, and local availability. The study proceeded from October 2020 to February 2023 in Egypt.

2 Methods

2.1 Plant material

Salvia officinalis L. herb was collected from South Sinai, Egypt, during Jun., 2020. The herb was kindly identified by Dr. Therese Labib, the chief consultant of Botanical Gardens in Egypt.

2.2 Biological material

Ad 7, hep-2 cells, H1N1 virus, and Vero E6 cells were provided from Nawah-Scientific, Egypt. The antibiotic & anti-mycotic solution, trypsin–EDTA, fetal bovine serum, and Dulbecco's Modified Eagle Medium (DMEM) were provided from Gibco BRL (USA). Chemicals as ethanol (Fisher Scientific UK), phosphate buffer tablets (PBS, pH 7.4, Bio Shop Canada Inc.), Tween 80, and cholesterol (Sigma Aldrich, USA) were used.

Animals Ninety Swiss Albino rats (210 ± 10 g; 60 for lethal dose (LD_{50}) determination & 30 for *S. officinalis* ethanol extract 70% anticancer activity) were obtained from the National Cancer Institute's animal house, Cairo University, Egypt. Rats were kept in an environmentally friendly environment, observed, and served with water and standard diet *ad libtum*.

2.3 Plant extraction

2.3.1 Preparation of S. officinalis ethanol extract

The maceration method [33] was used for the preparation of the ethanol extract 70% (SOEE). Powdered herb (350 g) was extracted in boiled ethanol 70% (1 L/ 3days/ 3 times) at room temperature.

2.4 Phytochemical analysis

2.4.1 Qualitative phytochemical screening

Phytochemical tests were done for SOEE using reference procedures [34, 35] to estimate its constituents. The screening was conducted on various substances, including terpenoids/steroids, saponins, carbohydrates, flavonoids, tannins, proteins/amino acids, and alkaloids [36–38].

2.4.2 Quantitative estimation of total phenolic & flavonoid contents

All tests were carried out spectrophotometrically utilizing the FluoStar Omega microplate reader, owing to settled standard calibration curves. The folin–Ciocalteau method was used to evaluate the total phenolic (TP) content [39], while the total flavonoid (TF) content was estimated by quantifying the color intensity formed when the aluminum chloride reagent made a complex with flavonoids [40]. According to Attard [41], the results were expressed as gallic acid (GAE) equivalents and rutin (RE) equivalents, respectively.

2.4.3 Quantitative estimation of total soluble carbohydrate (TSC) contents

The assay was conducted in accordance with the Gerhardt et al. method [42]. For the method in detail, see the Additional file 1: S1.

2.4.4 High-performance liquid chromatography (HPLC) analysis

The major phenolic constituents in the SOEE were characterized and identified by HPLC (Agilant 1260 series, Germany) combined with a diode array detector, depending on UV spectra and retention time. For descriptions of the analysis, see the Additional file 1: S2.

2.5 Isolation and identification of the Phenolic constituents

SOEE extract (1.5 g) was exposed to preparative separations using a PuriFlash 4100 system (Interchim Software 5.0, France). After collecting similar fractions and subfractions using paper chromatography (PC, 1MM), they were purified using preparative paper chromatography (3MM) and columns (Sephadex LH-20) [43]. Twelve compounds were isolated and subjected to structural elucidation using various investigative techniques: physical, chromatographic, and spectral analyses (ultra violet (UV), nuclear magnetic resonance (NMR), and mass spectrophotometer (MS) [44–46]. Also, all data obtained were compared with the previously reported values of identified compounds [47–49]. For a detailed method, see the Additional file 1: S3.

2.6 Biological activities

2.6.1 Antioxidant activity

2.6.1.1 DPPH assay The radical scavenging activity of SOEE was investigated by DPPH method developed by Boly et al. [50]. This method relies on reducing the color intensity of the DPPH reagent, measured at 540 ג nm [51]. Graph Pad Prism version 5 [52] was used for calculating IC_{50} values. The greater antioxidant power of the extract was indicated by the lower IC_{50} values. For more details, see the Additional file 1: S4.1.

2.6.1.2 FRAP assay The FRAP assay for SOEE was conducted using the previously mentioned method [53] with the use of microplates as a minor modification. The rapid reduction of ferrictripyridyltriazine (FeIII-TPTZ) and forming ferrous-tripyridyltriazine (FeII-TPTZ)

represent the power of the plant extract's antioxidant properties. The intensity of the blue color was measured by the microplate reader FluoStar Omega at 593 [51]. The increase in the iron reduction of the sample was indicated by the increase in absorbance. The results were expressed as μM Trolox equivalent per milligram sample (TE/mg sample) by utilizing the linear regression equation derived from the Trolox calibration curve (linear dose–response curve of Trolox).

2.6.1.3 ABTS assay The ABTS assay was established in accordance with the Arnao et al. method [54] using microplates as a minor modification. The results were expressed as μM TE/mg sample. For the concept and procedure in detail, see the Additional file 1: S4.2.

2.6.2 Antiviral activity

The potential antivirals against human Ad7 and H1N1 were assessed by the sulforhodamine B (SRB) assay and the crystal violet method, respectively. The cytotoxicity assays were demonstrated according to the recently reported cytopathic (CPE) inhibition effect [55, 56]. The efficacy of the antiviral was determined by dose–response assays; IC_{50} and CC_{50} (the range of cytotoxicity). Hep-2 cells and Vero E6 cells were cultured separately in a DMEM medium containing 10% fetal bovine serum and 0.1% antibiotic/antimycotic solution.

2.6.2.1 Human adenovirus type 7 (Ad7) To assess the cytotoxicity, hep-2 cells were used in the steps described for the assay of antiviral activity [57]. Calculating the cell viability percentage was based on the determination of Ad7 infectivity using the SRB method, which monitored CPE [55, 56]. see the Additional file 1: S5.

2.6.2.2 H1N1 virus (swine flu) The assessment of antiviral activity and cytotoxicity assays was conducted using the crystal violet technique [58]. Vero E6 cells were used for the cytotoxicity assay. The cell viability percentage was calculated by the determination of the influenza H1N1 infectivity through the monitoring of CPE using the crystal violet method. For detailed methods, see the Additional file 1: S6.

2.6.3 Cytotoxic activity

2.6.3.1 Determination of SOEE cytotoxicity on A549 lung carcinoma cell line The viability of A549cell lines was assessed by using MTT assay [59] for measuring the impact of SOEE, see the Additional file 1: S7.

2.6.4 In-vivo lung-protective activity of SOEE against $HgCl_2$-induced lung fibrosis

2.6.4.1 LD_{50} Determination for SOEE The LD_{50} was calculated by administering different doses of SOEE; 1200, 1800, 3000, 4000, 5000, and 6000 mg/kg to animal groups (n = 10) orally according to Maul et al. method [60]. The doses of the SOEE detected to be administrated to rats were 1/50 LD_{50}, 69.4 mg/kg.b.w. and 1/20 LD_{50}, 173.5 mg/kg.b.w. SOEE.

2.6.4.2 Experimental design Thirty adult male Swiss Albino rats weighing 200–220 gm were divided into five groups (n = 6/each) containing normal and treated rats. Group 1 was the negative control group, and its rats were administered distilled water (3ml/21 days). SOEE was suspended through distilled water and administrated by intragastric intubation. Group 2 administered SOEE (173.5 mg/k.g.) only, 3 times per week for 21 days. $HgCl_2$ (5 mg/ kg.b.w.) was administrated orally to group 3 to induce lung fibrosis in rats 3 times per week for 21 days [61]. Groups 4&5 were treated with $HgCl_2$ (5 mg/kg) and different doses of SOEE (69.4 mg/k.g./mL and 173.5 mg/k.g./mL, respectively). Blood samples were collected in heparinized tubes at 22nd day and centrifuged (1000 xg, 20 min). Total triglycerides (TG), cholesterol (TC), and cholesterol-high-density lipoprotein (HDL-C) levels were evaluated in the Plasma. Commercial kits (Asan and Youngdong Pharmaceutical Co., Korea) were used.

2.6.4.3 Lung specimens The lung tissue was homogenized in PBS (3 mL, pH 7.5) and then subjected to centrifugation (10 min, 3000 g). CAT, GSH, SOD, and TBARs were measured from the supernatant using a kit from Cayman Chemical Company (An Arbor, MI), while lung IL-1β, NF-κB, and COX-2 levels were assessed by an enzyme-linked immunosorbent assay (ELISA) kit from Shanghai YL Biotech Co. Ltd. (China).

2.6.4.4 Reverse transcription-quantitative polymerase chain reaction (RT-qPCR) The rats' lung tissues were used for the extraction of RNA under the method [62]. The method and the sequence of primers Table (1) used are discussed in detail in the Additional file 1: S8.

2.7 Statistical analysis

Results were reported as the mean ± standard deviation (SD) for six distinct spectrophotometric and ELISA measurements, in addition to three separate assessments for in vitro cytotoxicity and gene expression PCR analysis. The data were subjected to statistical analysis using

SPSS/20 software, employing ANOVA (one-way analysis of variance), followed by Bonferroni's multiple comparison test. *P-value* ($P < 0.01$) was considered to indicate statistical significance.

3 Results

3.1 Phytochemical analysis

3.1.1 Phytochemical screening tests

The results of the preliminary phytochemical screening tests listed in Table 1 showed the presence of a wide range of phytoconstituents such ascarbohydrates, phenolics, flavonoids, steroids and/or terpenoids, glycosides, tannins, and traces of alkaloids in the SOEE.

3.1.2 Yield, total phenolic, total flavonoid, and total soluble carbohydrate contents in the SOEE of S. officinalis herb

The yield of SOEE was 19 g/100 g herb powder. The estimation of TP, TF, and TC contents was possessed utilizing gallic acid, rutin, and glucose as references, respectively, through the linear regression equation of the calibration curve. The TP, TF, and TSC contents were 140.29 ± 0.9 mg GAE/g extract, 60.85 ± 0.6 mg RE/g extract, and 187.93 µg glucose/mg extract, respectively. It seems to be the first record of the total flavonoid amount and total carbohydrate contents of the Egyptian species.

3.1.3 HPLC analysis of SOEE 70% of S. officinalis L. Herb

Fourteen compounds were identified from HPLC analysis of SOEE, including nine phenolic acids and five flavonoids (Table 2). Rosmarinic and ferulic acids were the major phenolic compounds (326.7496% and 6.9838%), respectively. The major flavonoid constituents were luteolin aglycon (24.2018%) and luteolin-7-*O*-glucoside (18.5305%).

Table 1 Preliminary phytochemical screening tests of *S. officinalis* L. ethanol extract (70%) (SOEE)

Phyto-constituents	Results
Carbohydrates (Reducing sugars)	+ +
Phenolics	+ + +
Flavonoids	+ + +
Glycosides	+ +
steroids and/or terpenoids	+ +
Proteins/amino acids	+
Alkaloids	±
Tannins	+
Anthraquinones	–
Saponins	–
Cardiac glycosides	–

+ + + Abundant
± Traces
– Absent

Table 2 HPLC analysis of *S. officinalis* L. ethanol extract (70%) (SOEE)

No.	R_t	Compounds	Area%	Conc. (µg/g)
1	3.113	Gallic acid	1.2382	1370.00
2	3.848	Chlorogenic acid	3.0453	3387.98
3	5.273	Methyl gallate	0.8063	161.05
4	5.467	Caffeic acid	2.6854	663.66
5	5.816	Ellagic acid	3.3756	2066.20
6	7.543	Rutin	0.8239	1356.15
7	8.092	Syringic acid	0.4519	526.57
8	9.358	Luteolin-7-*O*-glucoside	18.5305	5778.87
9	9.542	Ferulic acid	6.9838	3520.93
10	9.916	Naringenin	0.7046	584.88
11	10.403	Luteolin	24.2018	
12	10.634	Rosmarinic acid	326.7496	
13	12.244	Taxifolin	0.1659	140.47
14	14.184	Kaempferol	0.5083	251.97

3.1.4 Characterization of the isolated compounds from SOEE

Chromatographic and spectroscopic analysis of the SOEE of sage approved the isolation and identification of twelve compounds (Fig. 1).: apigenin (1); luteolin(2), genkwanin (3), quercetin (4), hispidulin (5), luteolin-7-*O*-glucoside (6), quercetin-3-O-α- rhamnosyl ($1''' \rightarrow 6''$)-β-glucoside (rutin) (7), rosmarinic acid (8), caffeic acid (9), ferulic acid (10), chlorogenic acid (11), and ellagic acid (12). Dimethyl sulfoxide (DMSO)-d_6 was the solvent used for compound solubility in the ^{1}H-NMR.

Apigenin yellowish-white powder, m.p. 345-347 °C, soluble in ethyl acetate and methanol. It appeared as a strong purple fluorescence (λ254) and turned yellow with ammonia vapor which sharpened after spraying with 5% aluminum chloride ($AlCl_3$) reagent. Mass spectrum (EI-Ms) showed the molecular ion peak (M^+); m/z 270 corresponding to $C_{15}H_{10}O_5$ formula and fragments at 242, 213, 153, and 69 as major fragments. ^{1}H-NMR obtained results were similar to those published by Ateya et al. [63]. For data in detail, see the Additional file 1: S9.

Luteolin yellow powder, mp328–330 °C, soluble in ethyl acetate and methanol. It gives a strong purple fluorescence at λ254, 365 nm, which turned yellow with ammonia vapor, and the color was intensified by spraying with 5% $AlCl_3$ reagent. R_f value on PC; 0.49 (BAW, 4:1:5), 0.27, (CH_3COOH: H_2O; 1:1). EI-Ms spectrum: M^+; m/z 286 related to a molecular formula $C_{15}H_{10}O_6$ and fragments at m/z 258,153, 134 and 69 as major fragments. The data of UV spectra in methanol (MeOH): λ253, 296

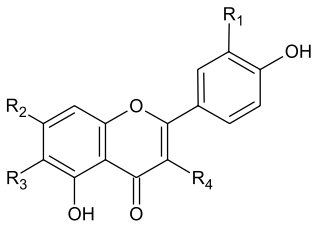

Apigenin	R_1 = H	R_2 = OH	R_3= H	R_4= H
Luteolin	R_1 = OH	R_2 = OH	R_3= H	R_4= H
Genkwanin	R_1 = H	R_2 = OCH_3	R_3= H	R_4= H
Quercetin	R_1 = OH	R_2 = OH	R_3= H	R_4= OH
Hispidulin	R_1 = H	R_2 = OH	R_3= OCH_3	R_4= H
Luteolin -7-*O*-*β*-glucopyranoside	R_1 = OH	R_2 = *O*-*β*-glucopyranoside	R_3= H	R_4= H
Rutin	R_1 = OH	R_2 = OH	R_3= H	R_4= *O*- rutinoside

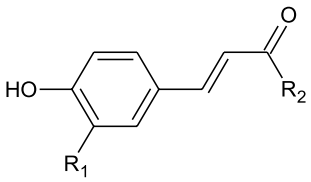

Caffeic acid	R_1= OH	R_2= OH
Ferulic acid	R_1= O-CH_3	R_2= OH
Chlorogenic acid	R_1= OH	R_2= quinic acid
Rosmarinic acid	R_1= OH	R_2= 3,4-dihydroxyphenyllactic acid

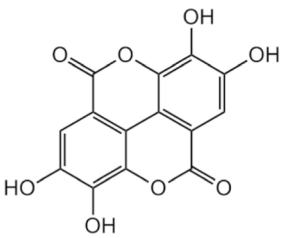

Ellagic acid

Fig. 1 Structures of isolated compounds (1–12) from *S. officinalis* L. (SOEE)

sh, 294 sh., 345. Sodium methoxide (NaOMe): λ272, 310 sh., 412. $AlCl_3$: 274, 300 sh., 328 sh.,420**.** $AlCl_3$/ HCl: 267, 297 sh., 353, 388. Sodium acetate (NaOAc): 267,310 sh., 75. NaOAc/H_3BO_3: 270, 297 sh., 362. Besides these, the^{1}H-NMR was similar to those published by Ateya et al. [63]. For data in detail, see the Additional file 1: S10.

Genkwanin yellow powder, mp278–280 °C, purple spot (UV; λ254, 365), yellow with ammonia and intensified with 5% aluminum chloride reagent, ^{1}H-NMR (DMSO -d_6, 500 MHz), δ 7.98 (^{1}H, d, 2'/6'-H, J=8.5 Hz), 6.98 (^{1}H, d, 3'/5'-H J=8.5 Hz), 6.81 (^{1}H, s,3-H), 6.85 (^{1}H, d,8-H), 6.44 (^{1}H, d,6-H), 3.85 (^{1}H, s,OCH_3-C7). EI- mass (m/z), 283(M^+), 267, 253, 167,152, 127, 62 (major peaks). The UV spectral data in methanol: λ 262, 340. NaOMe: λ 260,382. $AlCl_3$: 270, 297, 350, 390. $AlCl_3$/ HCl: 270, 297, 350, 390. NaOAc: 260,340. NaOAc/H_3BO_3: 262,330. Genkwanin was reported to have anti-tumor activity [64].

Quercetin yellow amorphous powder, mp 345–347 °C, soluble in ethyl acetate and methanol. It had a dark purple color (UV; λ254) and turned yellow with ammonia vapor. After spraying with 5% aluminum chloride

reagent, the color was intensified. EI-Ms spectrum exhibited the molecular ion peak (M^+) at m/z 270, representing a molecular formula $C_{15}H_{10}O_5$, and fragments at 242, 213, and 153, with 69 as major fragments. The ^{1}H-NMR (DMSO-d_6, 500 MHz) was the same as published by Amer et al. [51]. For data in detail, see the Additional file 1: S11.

Hispidulin yellow powder dissolved in methanol. The UV spectrum at MeOH (λmax, nm: 278, 336. The ^{1}H-NMR (DMSO-d_6, 400 MHz): δ 13.05 (1H, s, 5-OH), 10.88 (1H, s, 7-OH), 10.44 (1H, s, 4'-OH), 8.2 (2H, d, J = 8.4 Hz, H-2', 6'), 6.98 (2H, d, J = 8.4 Hz, H-3', 5'), 6.98 (1H, s, H-3), 6.65 (1H, s, H-8), 3.70 (3H, s, O-CH_3). The data were in agreement with previously reported for *Salvia plebeia* [48, 65]. It was identified before by LCMS/MS, but it is the first time to be isolated from the *S. officinalis* herb. Co-chromatography with a standard also confirmed the compound.

Luteolin-7-O-β- glucopyranoside yellow powder, soluble in methanol**,** mp 260–261 °C. The ^{1} H-NMR (DMSO -d_6, 500 MHz), aglycone: δ7.407 (^{1}H, m, 2'/6'-H), 6.88 (^{1}H, d, 5'-H, *J* = 8.5), 6.58 (^{1}H, s,3-H), 6.77, 6.47 (^{1}H, d, 6 /8-H), sugar moiety: 5.04 (^{1}H, d, H-1``, *J* = 7.5)**.** The UV spectral data in methanol: λ 253, 268(sh.), 347. NaOMe: λ 264, 403 $AlCl_3$: 273, 298 (sh.),427. $AlCl_3$/ HCl: 273, 296 (sh.), 354, 389. NaOAc: 265, 408. NaOAc/H_3BO_3: 263, 374. Acid hydrolysis was done and revealed the presence of aglycone (luteolin), and the sugar moiety was characterized by paper chromatography as glucose.

Rutin yellow amorphous powder, soluble in methanol, mp 240–242 °C, appeared as a dark purple spot under UV light (λ254, 365), and their yellow color appeared and intensified after being subjected to ammonia solution and spraying with 5% aluminum chloride reagent, respectively. The data of UV spectrophotometry and ^{1}H-NMR at DMSO-d_6 (400 MHz) were similar to that published by Amer et al., [51] in the identification of quercetin-3-O-rutinoside (rutin). For data in detail, see the Additional file 1: S12.

Rosmarinic acid yellowish white powder; the UV spectrum data (λmax, nm) at MeOH: 232, 329. EI-Ms spectrum exhibited (M^+) at m/z 361. ^{1}H-NMR (CD_3OD, 400 MHz): δ 7.56 (1H, d, *J* = 16 Hz, H7), 7.10 (1H, d, *J* = 2 Hz, H-2'), 6.95 (1H, dd, J = 8,2 Hz, H-6), 6.92 (1H, d, *J* = 8 Hz, H-5), 6.75 (1H, d, J = 8 Hz, H-5'), 6.75 (1H, d, *J* = 2 Hz, H-2), 6.69 (1H, dd, *J* = 8, 2 Hz, H-6'), 6.28 (1H, d, *J* = 16 Hz, H-8), 5.20 (1H, dd, J = 8.4, 4.4 Hz, H-8β), 3.11 (1H, dd, J = 14.2, 4.4 Hz, H-7β), 3.02 (1H, dd, J = 14.2, 8.4 Hz, H-7α); two doublets were found at 7.56 and 6.28 with large proton–proton coupling (J = 16 Hz) assigned to a pair of trans-olefinic protons, the same ABX system of three protons δ 3.02, 3.11 (*J* = 14) which represent H-7α& H-7β, and δ 5.20 (*J* = 8.4, 4.4 Hz, H-8β)). ^{13}C-NMR (CD_3OD, 100 MHz): δ 48.99 ppm (deuterated methanol), δ 127.4 (C-1), 115.3 (C-2), 146 (C-3), 146.6 (C-4), 122.7 (C-5), 116.4 (C-6), 37.6 (C-7), 74.8 (C-8), 172.3 (C-9), 129.1 (C-1'), 114.6 (C-2'), 144.8 (C-3'), 147.6 (C-4'), 123.8 (C-5'), 116.0 (C-6'), 148.2 (C-7'), 117.4 (C-8'), 167 (C-9'). The^{1}H NMR spectrum showed all data were in agreement with previously reported for *Salvia plebeia* [48, 65]. It identified before by LCMS/MS, but it is the first time to be isolated from *S. officinalis* herb.

Caffeic acid yellowish-brown powder, soluble in methanol, melting point (mp) 220 °C. It was appeared as blue fluorescence at UV(λ254), blue at (λ 365), and dark blue after spraying with ferric chloride reagent ($FeCl_3$), the UV (λmax, nm); (MeOH) (242, 296, 325) confirmed a phenyl propene skeleton [66]. ^{1}H-NMR (CD_3OD, 400 MHz) (δ ppm): δ 7.45 (1H, *d*, *J* = 16 Hz, H-7), 7.01 (1H, *d, J* = 2.1 Hz, H-2), 6.90 (1H, *dd*, *J* = 8, 2.1 Hz, H-6), 6.75 (^{1}H, *d*, *J* = 8 Hz, H-5), 6.2 (1H, *d*, *J* = 16 Hz, H-8). ^{13}C-NMR (CD_3OD, 100 MHz): δ 127(C-1), 115.8 (C-2), 146.3 (C-3), 148.6 (C-4), 121.8 (C-5), 114.3 (C-6), 145.8 (C-7), 114.6 (C-8), 170.3 (C-9). The data were similar to previously reported [67].

Ferulic acid off-white amorphous powder, it gave dark pot under short UV(λ254), and shiny violet under long UV (λ 365). ^{1}H-NMR (400 MHz) (δ ppm):, δ 7.49 (1H, *d*, *J* = 15.89, H-7), 7.08 (1H, *dd*,, *J* = 8.19, 1.93 Hz, H-6), 7.28 (1H, *d*, *J* = 1.9, H-2), 6.79 (1H, *d*, *J* = 8.06 Hz, H-5), 6.36 (^{1}H, *d*, *J* = 15.88 Hz, H-8), 3.7 (3H, *s,* O-CH_3).

Chlorogenic acid white powder**,** soluble in methanol, it´s melting point was 208–209 °C. It gave yellowish green fluorescence after the exposure of ammonia solution which turned to blue fluorescence after spraying with ferric chloride reagent. The results of ^{1}H-NMR (DMSO-d_6, 400 MHz), UV spectrum showed at methanol (MeOH), and co-chromatography was found to coincide with standard and with those previously published data for chlorogenic acid [68].

Ellagic acid white amorphous powder; the UV spectrum data at MeOH λ 255, 362. The ^{1}H NMR (DMSO, 400MHz); δ_{ppm}7.45 (2H, s, H-5, 5'). The compound was confirmed by co-chromatography with standard ellagic acid, and the obtained data were in agreement with that published by lil [69].

Table 3 Antioxidant activity of *S. officinalis* L. ethanol extract (70%) (SOEE)

	DPPH IC_{50} (ug/ mL)	FRAP (μM Trolox equivalent / mg extract)	ABTS
SOEE	23.21 ± 1.17	1864.71	1793.80
Trolox	42.42 ± 0.87	–	–

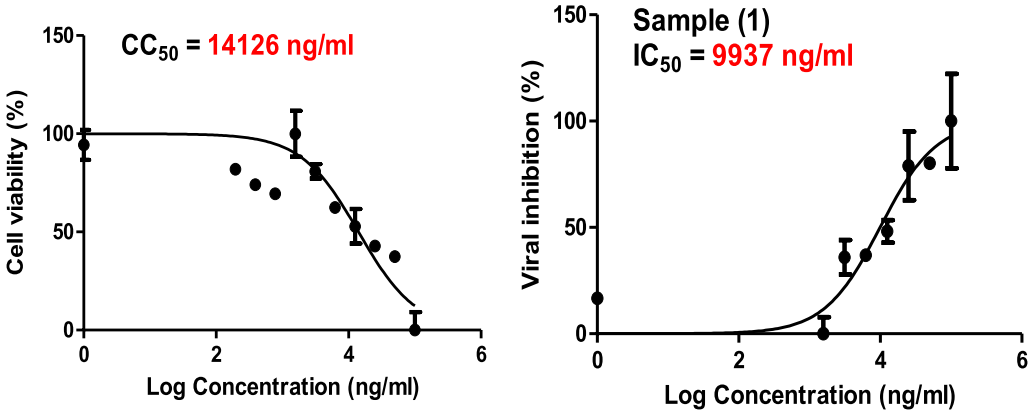

Fig. 2 Graphs of the cytotoxic concentration and inhibitory concentration of SOEE against *Adenovirus type* 7

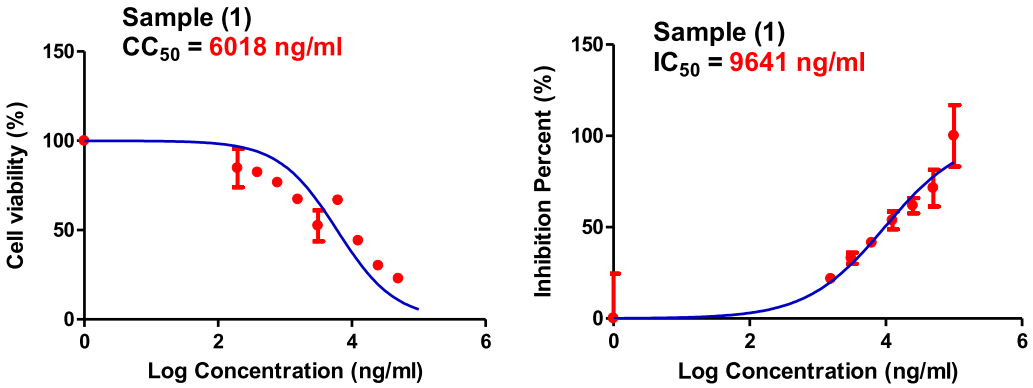

Fig. 3 Graphs of the cytotoxic concentration (CC_{50}) and inhibitory concentration (IC_{50}) of SOEE against Vero E6 cells and H1N1

3.2 Biological activities

3.2.1 Antioxidant activity: DPPH, FRAP, and ABTS.

DPPH, FRAP, and ABTS methods were utilized to examine the antioxidant activity of SOEE (Table 3). The IC_{50} for SOEE in the DPPH radical scavenging assay was 23.21 ± 1.17µg/mL compared with Trolox (IC_{50} 42.42 ± 0.87) as a standard antioxidant agent. As a role, the lower the IC_{50} value, the higher the antioxidant activity, while the values of the antioxidant activity quantified through FRAP and ABTS were 1864.71 and 1793.80 µM Trolox equivalent / mg extract, respectively. These data revealed that SOEE has highly antioxidant activity.

3.2.2 Antiviral activity

The determination of CC_{50} and IC_{50} for both Ad7 and H1N1 viruses was fulfilled using GraphPad PRISM software (Graph-Pad Software, San Diego, USA). The results are shown in Figs. 2 and 3, Table 4. Regarding Ad7, the IC_{50} of SOEE was 9.937µg/ml, and CC_{50} was14 µg/ml. Thus, IC_{50} of SOEE was lower than CC_{50} against adenovirus 7, which indicates a promising reduction of the virus concentration and more activity.

Table 4 Antiviral activity of *S. officinalis* L. (SOEE) against H1N1 and adenovirus (Ad7)

Antiviral	IC_{50} (ng/ mL)	CC_{50} (ng/ mL)
Ad7	9937	14126
H1N1	9641	6018

IC_{50} and CC_{50} of SOEE against H1N1 were 9.641 µg/ml and 6.018 µg/ml, respectively. The lowest reduction in H1N1 virus concentration indicated SOEE has less activity against H1N1 than Ad7. There were no reported data about the effect of ethanol extract of sage against these types of viruses.

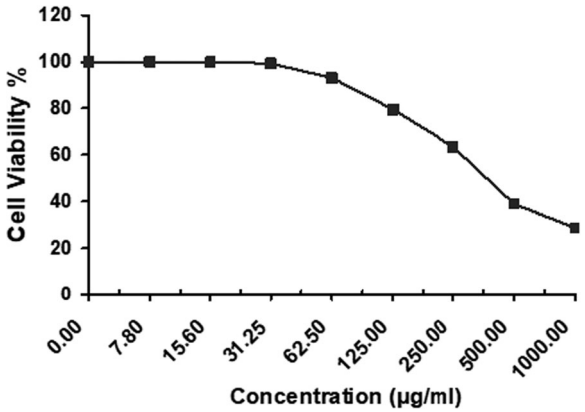

Fig. 4 IC_{50} value of SOEE against A549 lung cancer cell line

3.2.3 In vitro study

3.2.3.1 SOEE cytotoxicity SOEE had low IC_{50} value against the A549 lung cancer cell line. The results of MTT assay discussed that the SOEE incubation at different consternations (0, 7.8, 15.6, 31.25, 62.50, 125, 250, 500, and 1000 µg mL^{-1}) with A549 caused % of viability; 100, 100, 100, 99.26, 93.08, 79.54, 63.49, 39.02 and 28.75, respectively (Fig. 4), and toxicity % of 0, 0, 0, 0.74, 6.92, 20.46, 36.51, 60.98, and 71.25, respectively. The IC_{50} value of SOEE against A549 cancer cells was 387.9 µg/mL.

3.2.4 In vivo study

3.2.4.1 LD_{50} dose of SOEE in rats Oral administration of SOEE (10 rat/group) at doses 1200, 1800, 3000, 4000, 5000, and 6000 mg/kg b.w. resulted in mortalities 0, 1, 4, 7, 8, and 10, respectively. It was observed that the LD_{50} dose of SOEE was 3470 mg/kg b.w. Regarding the criteria, when the LD_{50} is greater than 2000 mg/kg, the plant extract is classified as relatively safe. The doses of SOEE administered to rats in the in vivo were determined with 1/50 LD_{50}, 69.4 mg/kg.b.w. and 1/20 LD_{50}, 173.5 mg/kg.b.w. SOEE.

3.2.4.2 Effect of SOEE on plasma TC, TG, and HDL-C levels The levels of TC, TG, and HDL-C are shown in Table 5. Oral administration of mercuric chloride ($HgCl_2$) at a dose (5 mg/kg b.w.) resulted in a significant increase in TC and TG levels to 46.95 and 74.96%, with a significant decrease in HDL-C level, 33.58%, compared to the control, which is evidence of lipid peroxidation.

Treatment by SOEE (69.4 mg/kg.b.w.) caused significantly reduction in the TC and TG levels to 27.28 and 27.15%, respectively, and elevation in HDL-C level significantly to 34.72%, comparing to the $HgCl_2$—treated group, while administration of SOEE (173.5 mg/kg.b.w.) to $HgCl_2$-treated rats led to a significant decrease at the TC and TG levels to 31.56 and 37.17%, respectively, with a significant increase in HDL-C level to 44.23%, on the plasma comparing to the group treated by $HgCl_2$.

3.2.4.3 Effect of SOEE on lung tissues SOD, CAT, GSH, and MDA Table 5 shows the levels of lung SOD, CAT, GSH, and MDA. The administration of $HgCl_2$ orally (5 mg/kg b.w.) led to a significant reduction in lung SOD, CAT, GSH, and MDA levels to 52.17%, 60.56%, 58.06%, and 146.15%, respectively, in comparison with the control group, indicating acute lung fibrosis. However, treatment with SOEE (69.4 mg/kg.b.w.) significantly elevated the lung SOD, CAT, and GSH levels to 55.06%, 66.75%, and 61.95%, with a significant decrease in lung MDA to 27.43%, respectively, comparing to the $HgCl_2$-treated group. Furthermore, the administration of SOEE (173.5 mg/kg.b.w.) to $HgCl_2$ -treated rats led to a significant increase in the level of lung SOD, CAT, and GSH to 114.02%, 185.43%, and 112.39%, as well as a significant decrease in the lung MDA level to 47.91%, compared to the $HgCl_2$- treated group. It can be concluded that the administration of SOEE orally provided remarkable protection against $HgCl_2$-induced lung damage [70].

3.2.4.4 Effect of SOEE on lung IL-1β, NF-κB, and COX-2 levels in treated rats Lung levels of IL-1β, NF-κB, and COX-2 in HgCl2-treated rats were dramatically increased by 99.89, 124.97, and 225.05%, respectively, as compared to normal rats (Table 5) ($p < 0.05$). Also, administration of SOEE (64.9 mg/kg.b.w.) to $HgCl_2$-treated rats produces a significant decrease in lung IL-1β, NF-κB, and COX-2 levels by 27.39, 24.78, and 32.49%, respectively, compared to $HgCl_2$-treated group ($p < 0.05$). Additionally, the administration of SOEE (173.5 mg/kg.b.w.) significantly decreased lung IL-1β, NF-κB, and COX-2 levels by 42.42, 44.19, and 56.51%, respectively, as compared to $HgCl_2$-exposed rats ($p < 0.05$).

Figure 5a, b shows that severe lung damage occurred in the $HgCl_2$-treated compared with the normal rats group. They had significant in lung Bcl-XL, Akt, and vanin-1 genes expression to 183, 152.68%, and 248.15%, respectively, as well as a decrease in lung P53 and Bcl-2 to 53.60 and 62.14%, respectively, compared with the control. After administration of SOEE at 69.4 mg/kg, lung Bcl-XL, Akt, and vanin-1 gene expression was significantly decreased to 18.37, 57.78, and 21.28%, respectively, and lung P53 and Bcl-2 was increased to 60.0 and 84.62%, respectively, comparing with $HgCl_2$. The administration of SOEE to $HgCl_2$ -treated rats at 173.5 mg/kg.b.w. announced a notable reduction in Bcl-XL, Akt, and vanin-1 genes expression of the lung to 50.88, 61.47, and 69.68%, respectively, as well as an increase in lung P53

Table 5 Effect of SOEE on levels of lipid, oxidative stress, and inflammation markers

Groups	Treatment Description	Lipid markers			Oxidative stress markers				Inflammation markers		
		TC (mg/dl)	TG (mg/dl)	HDL-C (mg/dl)	SOD (U/mg protein)	CAT (U/mg protein)	GSH (nmol/mg protein)	MDA (nmol/mg tissue)	IL-1β (ng/g tissue)	NF-κB (ng/g tissue)	COX-2 (ng/g tissue)
I	Negative control	133.27 ± 13.49^{a}	70.34 ± 5.40^{a}	29.27 ± 2.78^{b}	8.05 ± 0.73^{c}	18.46 ± 2.66^{c}	21.94 ± 3.29^{c}	1.17 ± 0.08^{a}	18.15 ± 2.79^{a}	12.05 ± 1.88^{a}	5.15 ± 0.74^{a}
II	SOEE (173.5 mg /k.g.)	134.90 ± 6.16^{a}	71.83 ± 6.21^{a}	30.84 ± 3.32^{b}	8.72 ± 0.64^{c}	21.64 ± 2.03^{c}	20.61 ± 1.47^{c}	1.14 ± 0.12^{a}	17.76 ± 3.26^{a}	11.80 ± 1.23^{a}	5.93 ± 0.86^{a}
III	$HgCl_2$ (5 mg/k.g.)	195.84 ± 18.57^{c}	123.07 ± 7.91^{d}	19.44 ± 2.82^{a}	3.85 ± 0.44^{a}	7.28 ± 1.38^{a}	9.20 ± 0.89^{a}	2.88 ± 0.26^{c}	36.28 ± 4.45^{c}	27.11 ± 2.85^{d}	16.74 ± 2.85^{c}
IV	SOEE (69.4 mg) + $HgCl_2$ (5 mg/kg.b.w.)	142.40 ± 9.85^{b}	89.66 ± 7.21^{c}	26.19 ± 4.58^{b}	5.97 ± 0.60^{b}	12.14 ± 1.97^{b}	14.90 ± 1.97^{b}	2.09 ± 0.25^{b}	26.34 ± 2.71^{b}	20.39 ± 2.44^{c}	11.30 ± 0.45^{b}
V	SOEE (173.5 mg) + $HgCl_2$ (5 mg/kg.b.w.)	134.02 ± 10.61^{a}	77.32 ± 6.58^{b}	28.04 ± 3.61^{b}	8.24 ± 0.40^{c}	20.78 ± 1.60^{c}	19.54 ± 1.13^{c}	1.50 ± 3.38^{a}	20.89 ± 3.90^{a}	15.13 ± 2.79^{b}	7.28 ± 0.60^{a}

Data show mean ± standard deviation of number of observations within each treatment. Data followed by the same letter are not significantly different at $P \leq 0.05$

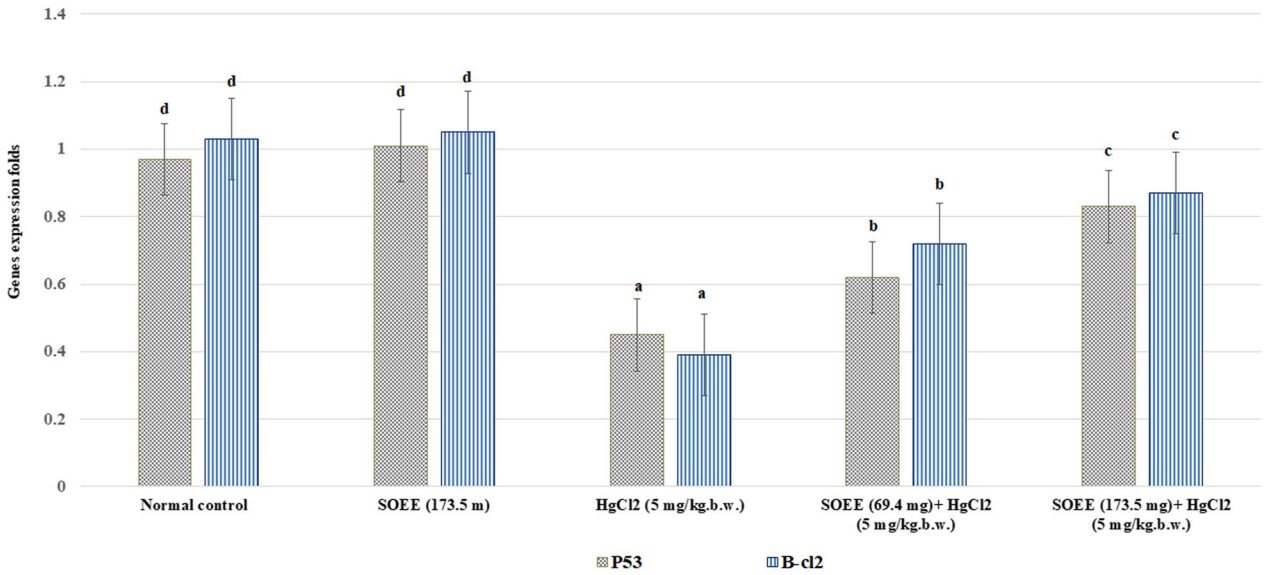

a. Effect of SOEE on lung P53 and Bcl-2 gene expression in control and treated rats.

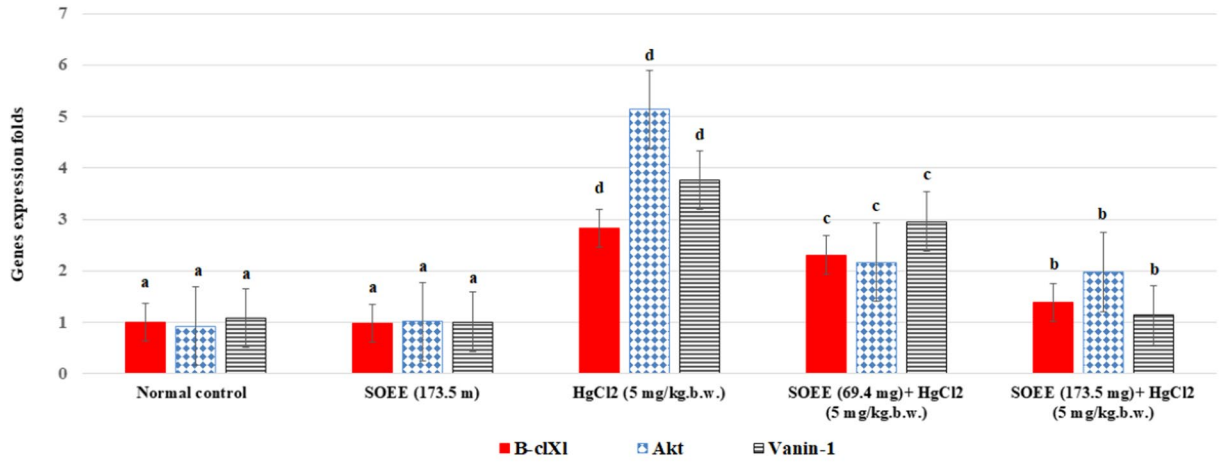

b. Effect of SOEE on lung Bcl-X_L, Akt and vanin-1 gene expression in treated rats.

Fig. 5 **a.** Effect of SOEE on lung P53 and Bcl-2 gene expression in control and treated rats. **b.** Effect of SOEE on lung Bcl-X_L, Akt and vanin-1 gene expression in treated rats

and Bcl-2 to 84.4 and 123.07% compared to rats administered $HgCl_2$.

4 Discussion

The preliminary phytochemical screening examinations proved to be helpful in the estimation of the bioactive components, which provided the herb with its beneficial characteristics and then made it easier to estimate them quantitatively. It was reported that the biological activities of sage are attributed to its phytoconstituents, including essential oils, phenolics (phenolic acids, flavonoids, and glycosides), terpenes, tannins, etc. [71]. The results of the yield obtained from the current study were consistent with those reported by Pereira et al. [72]. The qualitative estimation of the extract revealed the presence of different categories of phytoconstituents, which are consistent with the previously reported data by Ghorbani and Esmaeilizadeh [28]. Meanwhile, the quantitative estimation of the TP content record was particularly near to those reported by Afonso [71]. Naturally, the differences in the levels of phenolic were attributed to the climatic changes. There was no previous record regarding the quantitative determination of the TF contents

of this Egyptian species, *Salvia officinalis*, so our results seem to be the first record of the total flavonoid amount for this species. The Egyptian species contain TP and TF contents in more than ten folds of the species in Turkey [73]. Phenolics are responsible for a broad set of biological activities: antimicrobial, antioxidant, anti-inflammatory, and anticancer [28, 32, 74]. The data obtained from the quantitative estimation of the phenolic and flavonoid constituent of SOEE by HPLC were similar to those published by Herna´ndez [36], as rosmarinic and ellagic acids were the major phenolic acids but in different concentrations. The Egyptian herb contains 50-fold rosmarinic acid concentrations, and ellagic was nearly the same. Flavonoids and Phenolic acid concentrations might be influenced by some agricultural and climate factors [47]. Moreover, luteolin-7-*O*-glucoside and rosmarinic acid were the major phenolic acid and flavonoids in different countries [47, 49].

Herbal plants have a wide range of bioactive compounds with remarkable antioxidant properties, such as phenolic acids, flavonoids, catechins, and others. They are considered as a natural source of free-radical scavengers that protect the vital cells and organs from the dangerous effect of free radicals and remove reactive oxygen species (ROS) [75]. The antioxidant activity of major medicinal plants is strongly related to phenolic compounds (e.g., caffeic, rosmarinic, and carnosic acids). The twelve phenolic compounds isolated and identified from SOEE by chromatographic and spectroscopic techniques were previously identified in the plant by LC/MS/MS of *S. officinalis* L. herb and flowers [47–49]. It is the first record for the isolation of Hispidulin from this species.

Several studies reported that rosmarinic acid, caffeic acid, genkwanin, carnosol, carnosic acid, rosmanol, rosmadial, cirsimaritin, quercetin, and rutin are the most effective phenolic acids and flavonoids of *S. officinalis* [76, 77]. They protect cells from ROS-induced, lowering the risk of cancer, asthma, and fibrosis [78].

Oxidative stress has the main role in the development and progression of various diseases: diabetes, neurological diseases, cardiovascular disorders, bronchial asthma, and cancer [79, 80]. Normally, the body liberates free radicals through vital processes in a balance with naturally occurring scavengers such as glutathione. Excessive free radicals are liberated when this balance is out of control by age or injury, causing dangerous effects on cells and different diseases [81]. The authors used different methods with different mechanisms to determine the antioxidant capacity because only one method is insufficient and to obtain widely diverging results [82, 83].

In our study, the antioxidant activities of SOEE were powerful and relatively high. The low IC_{50} value for SOEE in the DPPH assay (23.21 ± 1.17μg/mL) represents twofold activities than Trolox (42.42 ± 0.87), therefore a high antioxidant activity. The reducing power (FRAP) and antioxidant ability of SOEE to reduce the ABTS were 1864.71 and 1793.80 μM Trolox equivalent /mg extract, respectively, that means it has 1.8- and 1.7-fold activities than Trolox. The obtained data were similar to that reported for DPPH of the *S. muirii* and *S. dolomitica* extracts [84] and 10 folds for ABTS than the other species. Our results were in agreement with the reported potent anti-oxidant activities of sage [76, 77].

The high content of phenolic constituents, especially rosmarinic acid, ellagic acid, caffeic acid derivative, chlorogenic acid as phenolic acids, and luteolin-7-O-glucopyranoside, quercetin, rutin as flavonoids, may be responsible for this powerful activity as that reported about their activities [77, 85]. In addition, phenolic constituents were responsible for other activities, such as the anti-inflammatory process, healing of pulmonary injury, and preventing pulmonary fibrosis [77]. It is the first report concerning the effect of SOEE as an antiviral.

Polyphenols have a significant impact on the prevention of cancer initiation and progression by employing diverse mechanisms. These mechanisms encompass the inhibition of oncogenes and genes associated with oxidative stress and inflammation [48, 65], as well as the modulation of epigenetic aberrations, including histone modifications, DNA methylations, and microRNAs [86]. Our phytochemical studies proved the presence of rosmarinic acid and ellagic acids in high concentrations in the SOEE formula, which were reported to have cytotoxic effects on cancer cells [56–61].

In the current study for acute toxicity, the administration of SOEE in different doses 1200, 1800, 3000, 4000, 5000, and 6000 mg/kg to animal groups (n = 10) orally didn't reveal any signs of mortality in all animals. Based on the documents provided by the Globally Harmonized System (GHS) of classification and labeling of chemicals, the substances having LD_{50} values greater than 2000 mg/kg are classified as relatively safe [87]. The use of such high doses as in previous studies of Nikitakis and Kowcz used 1290, 2020, 3200, or 5000 mg/kg b.w. for LD_{50} estimation of different plant extracts [88]. Regarding these criteria, SOEE was considered to be very safe. The doses of SOEE administered to rats in the in vivo were determined with 1/50 LD_{50}, 69.4 mg/kg.b.w. and 1/20 LD_{50}, 173.5 mg/kg.b.w. SOEE.

It is considered the first report to assess lung protection of SOEE on $HgCl_2$-induced lung damage in rats. $HgCl_2$ is a recognized substance that causes lung toxicity, principally through impairing the function of pulmonary surfactants [70]. A variety of signal transduction cascades are first activated in lung cells because of the host receptor first recognizing $HgCl_2$.

Several studies reported that $HgCl_2$ induced the production of ROS [63] and led to inflammation and a remarkable elevation in lung enzymes and lipid peroxidation [89, 90], as well as a significant rise in MDA and a decline in the activity of antioxidant enzymes in the lung [91]. This effect was compatible with Mohamed et al., who documented the increase in the inflammatory mediators' levels in rats administered with LPS [92, 93].

Based on these reports, our study observed substantial changes in lipid peroxidation (MDA) and IL-1β, NF-κB, and COX-2 levels. Additionally, there was a significant depletion of the pulmonary antioxidant system (SOD, CAT and GSH). Our study suggested that $HgCl_2$ causes oxidative damage to the lungs by inhibiting the NADPH oxidase pathway and reducing the levels of pulmonary SOD, CAT, and GSH in rats treated with $HgCl_2$. In addition, the Nrf-2/HO-1 pathway, which plays a crucial role in regulating the antioxidant system, was found to be imbalanced in lung tissues treated with $HgCl_2$. This imbalance resulted in the suppression of GSH and SOD activities, as well as the formation of O^{2-}, H_2O_2, NO, and iNos.

The administration of SOEE resulted in a hypolipidemic effect and inhibition of IL-1β, NF-κB, and COX-2, leading to a decrease in MDA levels and an increase in CAT, SOD, and GSH levels [94].

The improvements in SOD, CAT, and GSH levels, which play a critical biological function in eliminating ROS, are caused by SOEE's antioxidant and cell-protective activities [91, 95]. The current findings indicate that SOD, CAT, and GSH are activated by SOEE, which may aid in inhibiting the inflammatory reaction by lowering the oxidative stress brought on in rats treated with $HgCl_2$. Through several processes, SOEE may shield cellular components from $HgCl_2$ oxidative damage [96]. These include the up-regulation and activation of antioxidant enzymes, metal ion chelation, and ROS scavenging [97, 98].

The excessive production of MDA and inflammatory mediators (IL-1β, NF-κB, and COX-2) was associated with DNA damage. SOEE administration had a vital role in accelerating the repair of DNA. It is also considered a good protector of lung tissues. SOEE-treated rats had increased SOD and CAT activity, which resulted in decreased MDA production. GSH resynthesis also promotes DNA repair, which protects the lungs [99].

Our findings were consistent with previous studies that have demonstrated the efficacy of phenolic administration in reducing levels of IL-1β, NF-κB, and COX-2. This reduction in inflammatory markers leads to a decrease in lung inflammation and the generation of reactive oxygen species (ROS). Additionally, phenolics inhibit the expression of adhesion molecules and monocyte adhesion in lung tissue [100–104]. Antioxidant enzymes appear to be involved in this effect [105].

Our study predicted that the active phenolic compounds in SOEE, rosmarinic acid, caffeic acid, genkwanin, carnosol, carnosic acid, rosmanol, rosmadial, cirsimaritin, quercetin, and rutin, inhibit the production of IL-1β, NF-κB, and COX-2, prevent lung tissue degradation, protect cell membrane integrity, and delay inflammation. All these led to a reduction in lung fibrosis in HgCl2-treated rats' lungs.

The results of our study indicate that $HgCl_2$ decreased the expression of p53 and Bcl_2, as well as elevated the Bcl-XL, Akt, and vanin-1 gene expression in the lung of treated rats.

Furthermore, SOEE was found to be effective in significantly regulating biologically active lung P53, Bcl-X_L, Akt, and vanin-1 and induced Bcl-2 gene expression. Bcl-2 assumes a significant role in the development of fibrosis across various organs, such as lung fibrosis. It stimulates the production of collagen and fibronectin in fibroblasts [106]. Also, it has the ability to inhibit the protease production that degrades the extracellular matrix [107]. Bcl-2 has been found to be elevated in the alveolar inflammatory infiltrate of LPS-induced lung fibrosis [108].

In the current study, SOEE, as an antioxidant, plays its role in two levels. In the first level, eliminating ROS, preventing ROS synthesis, directly scavenging ROS, or controlling the activity of antioxidant enzymes, SOEE, eliminates ROS. SOEE stops the generation of ROS and inhibits ROS-producing enzymes at the second level [109].

SOEE could be demonstrating its anti-inflammatory activity through various mechanisms. Firstly, it can exert antioxidant and radical scavenging activities. Additionally, SOEE can modulate the metabolism of arachidonic acid by regulating enzymes such as cyclooxygenase, phospholipase A2, and lipoxygenase, thereby influencing the inflammatory response. Moreover, it can also affect the activity of nitric oxide synthase [110]. This protective effect is demonstrated by a decrease in the inflammatory response.

To the best of our knowledge, this is the first report highlighting the protective effect of SOEE against $HgCl_2$-induced pulmonary fibrosis. All the results fulfilled the objective and succeeded in proving the protective effect of *S. officinalis* from pulmonary fibrosis.

5 Conclusion

Salvia officinalis L. is considered one of the most powerful antioxidants, anti-inflammatory, and antiviral plants for their enrichment of phenolic acids and flavonoids, especially rosmarinic acid and luteolin-7-*O*-glucopyranisde. Also, we demonstrated that SOEE has a promising effect as an anti-inflammatory, healing the injury of the pulmonary after the viral infection and protecting from lung fibrosis. These effects organize us to expect the relation between SOEE-containing phenolics and flavonoid compounds and cytokines as well as oxidative stress biomarkers, which results in a modification in the inflammatory process associated with lung fibrosis. So, SOEE was suggested as an ideal herbal medicine in the treatment the lung injury and protects the lung from fibrosis.

Abbreviations

ABTS	3-Ethylbenzothiazoline-6-sulfonic acid
Ads7	Human adenoviruses type 7
$AlCl_3$	Aluminum chloride
BAW	Butanol: acetic acid: water
CAT	Catalase
CC_{50}	Cytotoxic concentration
CCID	Cell culture infective dose
CMV	Cytomegalovirus
COVID-19	Coronavirus
COX-2	Cyclooxygenase-2
CPE	Cytopathic effect
CPP1MM	Chromatographic paper chromatography (1MM)
DMEM	Dulbecco's modified eagle medium
DMSO	Dimethyl sulfoxide
DPPH	1,1-Diphenyl-2-picrylhydrazyl
EBV	Epstein–Barr virus
EDTA	Ethylenediaminetetraacetic acid
ELISA	Enzyme-linked immunosorbent assay
FeIII-TPTZ	Ferrictripyridyltriazine
FeII-TPTZ	Ferrous-tripyridyltriazine
FRAP	Ferric ion reducing antioxidant power
GAE	Gallic acid
GSH	Glutathione
H1N1	Human influenza subtype 1 (swine flu)
H_3BO_3	Boric acid
HCV	Hepatitis C virus
HDL-C	High-density lipoprotein
$HgCl_2$	Mercuric chloride
HIV	Human immunodeficiency virus
HOAc	Acetic acid
HPLC	High-performance liquid chromatography
HTLV	Human T-cell leukemia virus
IC_{50}	Inhibitory concentration
IL-1β	Interleukin-1β
LD_{50}	Lethal dose
LF	Lung fibrosis
MDA	Malondialdehyde
MeOH	Methanol
MERS-CoV	Middle East respiratory syndrome
MHV-68	Murine γ-herpes virus 68
mp	Melting point
MS	Mass spectrophotometer
NaOAc	Sodium acetate
NaOMe	Sodium methoxide
NF-κB	Necrosis factor kappa
NMR	Nuclear magnetic resonance
OD	Optical density
PBS	Phosphate-buffered saline
PCR	Polymerase chain reaction
PF	Pulmonary fibrosis
RE	Rutin
SARS	Severe acute respiratory syndrome
SOD	Superoxide dismutase
SOEE	*Salvia officinalis* ethanol extract
SRB	Sulforhodamine B
TBARs	Thiobarbituric acid reactive substances
TC	Total cholesterol
TF	Total flavonoids
TG	Triglycerides
TP	Total phenolics
TSC	Total carbohydrates
UV	Ultraviolet
VI	Viral infections
WHO	World Health Organization

Supplementary Information

The online version contains supplementary material available at https://doi.org/10.1186/s43088-024-00498-6.

Additional file 1. Additional file 1 of Chemical composition, antioxidant, cytotoxic, antiviral and lung protective activities of Salvia officinalis L. ethanol extract herb growing in Sinai, Egypt.

Acknowledgements
Not applicable

Author contributions
AA involved in conceptualization, methodology, data curation, formal analysis, investigation, writing–original draft, writing–review and editing. SK took part in methodology, visualization, writing–original draft. M.H involved in conceptualization, formal analysis, investigation, methodology, writing–original draft. All authors have read and agreed to the published version of the manuscript**.**

Funding
This research received no external funding.

Availability of data and material
All relevant data are within the paper and its supplementary information files. Any other data would be available from the corresponding author upon reasonable request.

Declarations

Ethical approval and consent to participate
The experimental procedures were approved by the Ethical Committee of the National Research Centre, Dokki, Egypt (approval No. 043042021).

Consent for publication
Not applicable.

Competing interest
There is no conflict of interest. The authors declare that the research was conducted in the absence of any commercial or financial relationships.

Author details
[1]Department of Pharmacognosy Pharmaceutical and Drug Industries Research Institute, National Research Centre, Dokki, Cairo 12622, Egypt. [2]Biochemistry Department, Faculty of Applied Health Sciences Technology, October 6 University, Sixth of October City, Egypt. [3]Biotechnology Department, Faculty of Applied Health Sciences Technology, October 6 University, Sixth of October City, Egypt.

Received: 20 February 2024 Accepted: 24 April 2024
Published online: 30 April 2024

References

1. Huang WJ, Tang XX (2021) Virus infection induced pulmonary fibrosis. J Transl Med 19:1–15
2. Tran S, Ksajikian A, Overbey J, Li P, Li Y (2022) Pathophysiology of pulmonary fibrosis in the context of COVID-19 and implications for treatment: a narrative review. Cells 11:2489
3. Gentile F, Aimo A, Forfori F, Catapano G, Clemente A, Cademartiri F, Emdin M, Giannoni A (2020) COVID-19 and risk of pulmonary fibrosis: the importance of planning ahead. Eur J Prev Cardiol 27:1442–1446
4. Naik PK, Moore BB (2010) Viral infection and aging as cofactors for the development of pulmonary fibrosis. Expert Rev Respir Med 4:759–771
5. Ueda T, Ohta K, Suzuki N, Yamaguchi M, Hirai K, Horiuchi T, Watanabe J, Miyamoto T, Ito K (1992) Idiopathic pulmonary fibrosis and high prevalence of serum antibodies to hepatitis C virus1• 2. Am Rev Respir Dis 1:268
6. Wilson MS, Wynn TA (2009) Pulmonary fibrosis: pathogenesis, etiology and regulation. Mucosal Immunol 2:103–121
7. De Jong JC, Wermenbol AG, Verweij-Uijterwaal MW, Slaterus KW, Wertheim-Van Dillen P, Van Doornum GJJ, Khoo SH, Hierholzer JC (1999) Adenoviruses from human immunodeficiency virus-infected individuals, including two strains that represent new candidate serotypes Ad50 and Ad51 of species B1 and D, respectively. J Clin Microbiol 37:3940–3945
8. Jilani TN, Jamil RT, Siddiqui AH (2018) H1N1 influenza
9. World Health Organization (2020) Coronavirus disease 2019 (COVID-19): situation report, 99
10. Kant A, Kostakoğlu U, Saral ÖB, Çomoğlu Ş, Arslan M, Karakoç HN, Erkan G, Ertunç B, Demir HD, Aydin M et al (2021) Comparison of two pandemics: H1N1 and SARS-CoV-2. Rev Assoc Med Bras 67:115–119
11. Betteridge DJ (2000) What is oxidative stress? Metabolism 49:3–8
12. Ighodaro OM, Akinloye OA (2018) First line defence antioxidants-superoxide dismutase (SOD), catalase (CAT) and glutathione peroxidase (GPX): their fundamental role in the entire antioxidant defence grid. Alex J Med 54:287–293
13. Bezerra FS, Lanzetti M, Nesi RT, Nagato AC, Silva CP, Kennedy-Feitosa E, Melo AC, Cattani-Cavalieri I, Porto LC, Valenca SS (2023) Oxidative stress and inflammation in acute and chronic lung injuries. Antioxidants 12:548
14. Hussein MA (2013) Prophylactic effect of resveratrol against ethinylestradiol-induced liver cholestasis. J Med Food 16:246–254
15. Mohammed Abdalla H, Soad Mohamed AG (2010) In vivo hepatoprotective properties of purslane extracts on paracetamol-induced liver damage. Malays J Nutr 16:161–170
16. Saddam M, Paul SK, Habib MA, Fahim MA, Mimi A, Islam S, Paul B, Helal MMU (2024) Emerging biomarkers and potential therapeutics of the BCL-2 protein family: the apoptotic and anti-apoptotic context. Egypt J Med Hum Genet 25:12
17. Korsmeyer SJ, Shutter JR, Veis DJ, Merry DE, Oltvai ZN (1993) Bcl-2/Bax: a rheostat that regulates an anti-oxidant pathway and cell death. In: Seminars in cancer biology. pp 327–332
18. Hardwick JM, Soane L (2013) Multiple functions of BCL-2 family proteins. Cold Spring Harb Perspect Biol 5:a008722
19. Bartucci R, Salvati A, Olinga P, Boersma YL (2019) Vanin 1: its physiological function and role in diseases. Int J Mol Sci 20:3891
20. Mostafa MM, Amin MM, Zakaria MY, Hussein MA, Shamaa MM, Abd El-Halim SM (2023) Chitosan surface-modified PLGA nanoparticles loaded with cranberry powder extract as a potential oral delivery platform for targeting colon cancer cells. Pharmaceutics 15:606
21. Kennedy SG, Kandel ES, Cross TK, Hay N (1999) Akt/Protein kinase B inhibits cell death by preventing the release of cytochrome c from mitochondria. Mol Cell Biol 19:5800–5810
22. Tamokou JD, Chouna JR, Fischer-Fodor E, Chereches G, Barbos O, Damian G, Benedec D, Duma M, Efouet APN, Wabo HK et al (2013) Anticancer and antimicrobial activities of some antioxidant-rich Cameroonian medicinal plants. PLoS One 8:e55880
23. Nguanchoo V, Balslev H, Sadgrove NJ, Phumthum M (2023) Medicinal plants used by rural Thai people to treat non-communicable diseases and related symptoms. Heliyon 9:e12758
24. da Costa FE, Anselmo MD, Guerra NM, de Lucena CM, Felix CD, Bussmann RW, Paniagua-Zambrana NY, de Lucena RFP et al (2021) Local knowledge and use of medicinal plants in a rural community in the Agreste of Paraíba, Northeast Brazil. Evid Based Complement Altern Med. https://doi.org/10.1155/2021/9944357
25. Alqahtani LS, Abd-Elhakim YM, Mohamed AA-R, Khalifa NE, Khamis T, Alotaibi BS, Alosaimi M, El-Kholy SS, Abuzahrah SS, ElAshmouny N et al (2023) Curcumin-loaded chitosan nanoparticles alleviate fenpropathrin-induced hepatotoxicity by regulating lipogenesis and pyroptosis in rats. Food Chem Toxicol 180:114036
26. Salem GA, Mohamed AA-R, Khater SI, Noreldin AE, Alosaimi M, Alansari WS, Shamlan G, Eskandrani AA, Awad MM, El-Shaer RAA et al (2023) Enhancement of biochemical and genomic pathways through lycopene-loaded nano-liposomes: alleviating insulin resistance, hepatic steatosis, and autophagy in obese rats with non-alcoholic fatty liver disease: involvement of SMO, GLI-1, and PTCH-1 genes. Gene 883:147670
27. Writer CIR (2021) Safety assessment of salvia officinalis (Sage)-derived ingredients as used in cosmetics
28. Ghorbani A, Esmaeilizadeh M (2017) Pharmacological properties of Salvia officinalis and its components. J Tradit Complement Med 7:433–440
29. Czygan F-C (2004) Herbal drugs and phytopharmaceuticals: a handbook for practice on a scientific basis. CRC Press, Boca Raton
30. Staff TPDR (2004) PDR for herbal medicines. Physician's Desk Reference (PDR)
31. Vogel A, Finder P, Freshness S (2015) Plant Encyclopaedia.'. Aristolochia clematitis
32. Thorsen MA, Hildebrandt KS (2003) Quantitative determination of phenolic diterpenes in rosemary extracts: aspects of accurate quantification. J Chromatogr A 995:119–125
33. Ollanketo M, Peltoketo A, Hartonen K, Hiltunen R, Riekkola M-L (2002) Extraction of sage (*Salvia officinalis* L.) by pressurized hot water and conventional methods: antioxidant activity of the extracts. Eur Food Res Technol 215:158–163
34. Harborne AJ (1998) Phytochemical methods a guide to modern techniques of plant analysis. Springer Science \& Business Media, Berlin
35. Fischer NH, Isman MB, Stafford HA (2012) Modern phytochemical methods. Springer Science \& Business Media, Berlin
36. Parekh J, Chanda S (2007) In vitro antimicrobial activity and phytochemical analysis of some Indian medicinal plants. Turk J Biol 31:53–58
37. Prabhu K, Karar PK, Hemalatha S, Ponnudurai K et al (2011) A comparative preliminary phytochemical screening on the leaves, stems and the roots of three Viburnum Linn. species. Der Pharmacia Sin 2:81–93
38. Shinde PR, Patil PS, Bairagi VA (2012) Pharmacognostic, phytochemical properties and antibacterial activity of Callistemon citrinus viminalis leaves and stems. Int J Pharm Pharm Sci 4:406–408
39. Asadi S, Ahmadiani A, Esmaeili MA, Sonboli A, Ansari N, Khodagholi F (2010) In vitro antioxidant activities and an investigation of neuroprotection by six Salvia species from Iran: a comparative study. Food Chem Toxicol 48:1341–1349
40. Kiranmai M, Kumar CBM, Mohammed I et al (2011) Comparison of total flavanoid content of Azadirachta indica root bark extracts prepared by different methods of extraction. Res J Pharm Biol Chem Sci 2:254–261
41. Attard E (2013) A rapid microtitre plate Folin-Ciocalteu method for the assessment of polyphenols. Open Life Sci 8:48–53
42. Gerhardt P, Murray RGE, Wood WA, Krieg NR (1994) Methods for general and molecular bacteriology. American Society for Microbiology, Washington, DC. Stackebrandt E, Goebel BM 607654
43. Lomas-Soria C, Pérez- Ramírez IF, Caballero-Pérez J, Guevara-Gonzalez RG, Guevara-Olvera L, Loarca-Piña G, Guzman-Maldonado HS, Reynoso-Camacho R (2015) Cooked common beans (*Phaseolus vulgaris* L.) modulate renal genes in streptozotocin-induced diabetic rats. J Nutr Biochem 26:761–768
44. Agrawal PK (1989) Flavonoids. Carbon-13 NMR of flavonoids 564:
45. Markham KR et al (1982) Techniques of flavonoid identification. Academic Press, Cambridge
46. Mabry T, Markham KR, Thomas MB (2012) The systematic identification of flavonoids. Springer Science \& Business Media, Berlin
47. Areias F, Valentão P, Andrade PB, Ferreres F, Seabra RM (2000) Flavonoids and phenolic acids of sage: influence of some agricultural factors. J Agric Food Chem 48:6081–6084
48. Hernández-Saavedra D, Pérez-Ramírez IF, Ramos-Gómez M, Mendoza-Díaz S, Loarca-Piña G, Reynoso-Camacho R (2016) Phytochemical characterization and effect of *Calendula officinalis*, *Hypericum perforatum*,

and *Salvia officinalis* infusions on obesity-associated cardiovascular risk. Med Chem Res 25:163–172. https://doi.org/10.1007/s00044-015-1454-1
49. Gericke S, Lübken T, Wolf D, Kaiser M, Hannig C, Speer K (2018) Identification of new compounds from sage flowers (*Salvia officinalis* L.) as markers for quality control and the influence of the manufacturing technology on the chemical composition and antibacterial activity of sage flower extracts. J Agric Food Chem 66:1843–1853
50. Boly R, Lamkami T, Lompo M, Dubois J, Guissou I (2016) DPPH free radical scavenging activity of two extracts from Agelanthus dodoneifolius (Loranthaceae) leaves. Int J Toxicol Pharmacol Res 8:29–34
51. Amer AA, Mohammed RS, Hussein Y, Ali ASM, Khalil AA (2022) Development of Lepidium sativum extracts/PVA electrospun nanofibers as wound healing dressing. ACS Omega 7:20683–20695. https://doi.org/10.1021/acsomega.2c00912
52. Chen Z, Bertin R, Froldi G (2013) EC50 estimation of antioxidant activity in DPPH assay using several statistical programs. Food Chem 138:414–420
53. Benzie IFF, Strain JJ (1996) The ferric reducing ability of plasma (FRAP) as a measure of "antioxidant power": the FRAP assay. Anal Biochem 239:70–76. https://doi.org/10.1006/abio.1996.0292
54. Arnao MB, Cano A, Acosta M (2001) The hydrophilic and lipophilic contribution to total antioxidant activity. Food Chem 73:239–244
55. Song J-H, Choi H-J, Song H-H, Hong E-H, Lee B-R, Oh S-R, Choi K, Yeo S-G, Lee Y-P, Cho S et al (2014) Antiviral activity of ginsenosides against coxsackievirus B3, enterovirus 71, and human rhinovirus 3. J Ginseng Res 38:173–179
56. Choi H-J, Kim J-H, Lee C-H, Ahn Y-J, Song J-H, Baek S-H, Kwon D-H (2009) Antiviral activity of quercetin 7-rhamnoside against porcine epidemic diarrhea virus. Antiviral Res 81:77–81
57. Vichai V, Kirtikara K (2006) Sulforhodamine B colorimetric assay for cytotoxicity screening. Nat Protoc 1:1112–1116
58. Schmidtke M, Schnittler U, Jahn B, Dahse H-M, Stelzner A (2001) A rapid assay for evaluation of antiviral activity against coxsackie virus B3, influenza virus A, and herpes simplex virus type 1. J Virol Methods 95:133–143
59. Mosmann T (1983) Rapid colorimetric assay for cellular growth and survival: application to proliferation and cytotoxicity assays. J Immunol Methods 65:55–63
60. Maul JD, Blackstock C, Brain RA (2018) Derivation of avian dermal LD50 values for dermal exposure models using in vitro percutaneous absorption of [14C]-atrazine through rat, mallard, and northern bobwhite full thickness skin. Sci Total Environ 630:517–525
61. Abarikwu SO, Benjamin S, Ebah SG, Obilor G, Agbam G (2017) Protective effect of Moringa oleifera oil against HgCl2-induced hepato-and nephro-toxicity in rats. J Basic Clin Physiol Pharmacol 28:337–345
62. Livak KJ, Schmittgen TD (2001) Analysis of relative gene expression data using real-time quantitative PCR and the 2- $Δ$$Δ$CT method. Methods 25:402–408
63. Ateya A, Ammar N, El-Eraky W, El-Senousy W, El Awdan S, Amer A et al. Antiviral, cytotoxicity, antioxidant and chemical constituents of Adansonia digitata grown in Egypt
64. Cong Y, Guo J, Wang T, Li M, Li K, Wang J, Li Q (2009) Chemical constituents and antitumor activity on leukemia K562 cell of Leonurus heterophyllus. Zhongguo Zhong Yao Za Zhi 34:1816–1818
65. Lee GT, Duan CH, Lee J-N, Lee K-S, Hong J-T, Lee K-K (2010) Phytochemical constituents from Salvia plebeia. Nat Prod Sci 16:207–210
66. Williams CA, Harborne JB (1986) Flavone and flavonol glycosides. The flavonoids: advances in research since 337–385
67. Lee I-C, Bae J-S, Kim T, Kwon OJ, Kim TH (2011) Polyphenolic constituents from the aerial parts of Thymus quinquecostatus var. japonica collected on Ulleung Island. J Korean Soc Appl Biol Chem 54:811–816
68. Suárez-Quiroz ML, Alonso Campos A, Valerio Alfaro G, González-Ríos O, Villeneuve P, Figueroa-Espinoza MC (2014) Isolation of green coffee chlorogenic acids using activated carbon. J Food Compos Anal 33:55–58. https://doi.org/10.1016/j.jfca.2013.10.005
69. Li X-C, Elsohly HN, Hufford CD, Clark AM (1999) NMR assignments of ellagic acid derivatives. Magn Reson Chem 37:856–859
70. Ismail OI, El-Meligy MMS (2021) Could vitamin C protect against mercuric chloride induced lung toxicity in the offspring rat: a histological and immunohistochemical study. Ultrastruct Pathol 45:197–211
71. Afonso AF, Pereira OR, Fernandes Â, Calhelha RC, Silva AMS, Ferreira ICFR, Cardoso SM (2019) Phytochemical composition and bioactive effects of Salvia africana, Salvia officinalis 'Icterina'and Salvia mexicana aqueous extracts. Molecules 24:4327
72. Pereira OR, Catarino MD, Afonso AF, Silva AMS, Cardoso SM (2018) Salvia elegans, Salvia greggii and Salvia officinalis decoctions: Antioxidant activities and inhibition of carbohydrate and lipid metabolic enzymes. Molecules 23:3169
73. Erdoğan SS, Karik Ü, Başer KH (2014) The determination of antioxidant activity of some sage populations of in the Marmara region. Türk Tarım ve Doğa Bilimleri Dergisi 1:1877–1882
74. Baricevic D, Sosa S, Della Loggia R, Tubaro A, Simonovska B, Krasna A, Zupancic A (2001) Topical anti-inflammatory activity of *Salvia officinalis* L. leaves: the relevance of ursolic acid. J Ethnopharmacol 75:125–132
75. Singh M, Govindarajan R, Nath V, Rawat AKS, Mehrotra S (2006) Antimicrobial, wound healing and antioxidant activity of Plagiochasma appendiculatum Lehm. et Lind. J Ethnopharmacol 107:67–72
76. Cuvelier M-E, Richard H, Berset C (1996) Antioxidative activity and phenolic composition of pilot-plant and commercial extracts of sage and rosemary. J Am Oil Chem Soc 73:645–652
77. Cuvelier ME (2002) Antioxidative activity and phenolic composition of pilot-plant and commercial extracts of sage and rosemary. JAOCS 162:981–987
78. Kaurinovic B, Vastag D (2019) Flavonoids and phenolic acids as potential natural antioxidants. IntechOpen London, UK
79. Li H, Horke S, Förstermann U (2013) Oxidative stress in vascular disease and its pharmacological prevention. Trends Pharmacol Sci 34:313–319
80. Salazar R, Pozos ME, Cordero P, Perez J, Salinas MC, Waksman N (2008) Determination of the antioxidant activity of plants from Northeast Mexico. Pharm Biol 46:166–170
81. Jayaprakasha GK, Singh RP, Sakariah KK (2001) Antioxidant activity of grape seed (Vitis vinifera) extracts on peroxidation models in vitro. Food Chem 73:285–290
82. Frankel EN, Meyer AS (2000) The problems of using one-dimensional methods to evaluate multifunctional food and biological antioxidants. J Sci Food Agric 80:1925–1941
83. Huang D, Ou B, Prior RL (2005) The chemistry behind antioxidant capacity assays. J Agric Food Chem 53:1841–1856
84. Kamatou GPP, Viljoen AM, Steenkamp P (2010) Antioxidant, antiinflammatory activities and HPLC analysis of South African Salvia species. Food Chem 119:684–688
85. Wang M, Li J, Rangarajan M, Shao Y, LaVoie EJ, Huang T-C, Ho C-T (1998) Antioxidative phenolic compounds from sage (*Salvia officinalis*). J Agric Food Chem 46:4869–4873
86. Bujak T, Zagórska-Dziok M, Ziemlewska A, Nizioł-Łukaszewska Z, Wasilewski T, Hordyjewicz-Baran Z (2021) Antioxidant and cytoprotective properties of plant extract from dry flowers as functional dyes for cosmetic products. Molecules 26:2809
87. Philpot R (2011) The purple book. Biteback Publishing, Hull
88. Nikitakis J, Kowcz A (2019) Web-based international cosmetic ingredient dictionary and handbook (wINCI Dictionary)
89. Ali S, Awan Z, Mumtaz S, Shakir HA, Ahmad F, Ulhaq M, Tahir HM, Awan MS, Sharif S, Irfan M et al (2020) Cardiac toxicity of heavy metals (cadmium and mercury) and pharmacological intervention by vitamin C in rabbits. Environ Sci Pollut Res 27:29266–29279
90. Liu B, Yu H, Baiyun R, Lu J, Li S, Bing Q, Zhang X, Zhang Z (2018) Protective effects of dietary luteolin against mercuric chloride-induced lung injury in mice: involvement of AKT/Nrf2 and NF-$κ$B pathways. Food Chem Toxicol 113:296–302
91. Sun S, Fu J, Liu K, Dai M, Li Y, Liu Y, Ma S, Qu J (2021) Two new iridoid glucosides from the whole plant of patrinia scabiosifolia link. Molecules 26:4201
92. Mohamad EA, Fahmy HM (2020) Niosomes and liposomes as promising carriers for dermal delivery of Annona squamosa extract. Braz J Pharm Sci 56:e18096
93. Mohamad EA, Aly AA, Khalaf AA, Ahmed MI, Kamel RM, Abdelnaby SM, Abdelzaher YH, Sedrak MG, Mousa SA (2021) Evaluation of natural bioactive-derived punicalagin niosomes in skin-aging processes accelerated by oxidant and ultraviolet radiation. Drug Des Develop Ther 15:3151–3162

94. Zhang Y, Guo H, Cheng BC-Y, Su T, Fu X-Q, Li T, Zhu P-L, Tse K-W, Pan S-Y, Yu Z-L (2018) Dingchuan tang essential oil inhibits the production of inflammatory mediators via suppressing the IRAK/NF-$κ$B, IRAK/AP-1, and TBK1/IRF3 pathways in lipopolysaccharide-stimulated RAW264.7 cells. Drug Des Develop Ther 12:2731–2748
95. Craig R, Larkin A, Mingo AM, Thuerauf DJ, Andrews C, McDonough PM, Glembotski CC (2000) p38 MAPK and NF-$κ$B collaborate to induce interleukin-6 gene expression and release: evidence for a cytoprotective autocrine signaling pathway in a cardiac myocyte model system. J Biol Chem 275:23814–23824
96. Ehrentraut H, Weisheit CK, Frede S, Hilbert T (2019) Inducing acute lung injury in mice by direct intratracheal lipopolysaccharide instillation. JoVE (J Vis Exp) 6:e59999
97. Baradaran Rahimi V, Rakhshandeh H, Raucci F, Buono B, Shirazinia R, Samzadeh Kermani A, Maione F, Mascolo N, Askari VR (2019) Anti-inflammatory and anti-oxidant activity of Portulaca oleracea extract on LPS-induced rat lung injury. Molecules 24:139
98. Gui T, Sun Y, Shimokado A, Muragaki Y (2012) The roles of mitogen-activated protein kinase pathways in TGF-$β$-induced epithelial-mesenchymal transition. J Signal Transduct. https://doi.org/10.1155/2012/289243
99. Clementi ME, Pani G, Sampaolese B, Tringali G (2018) Punicalagin reduces H2O2-induced cytotoxicity and apoptosis in PC12 cells by modulating the levels of reactive oxygen species. Nutr Neurosci 21:447–454
100. Khorsandi K, Kianmehr Z, Hosseinzadeh R et al (2020) Anti-cancer effect of gallic acid in presence of low level laser irradiation: ROS production and induction of apoptosis and ferroptosis. Cancer Cell Int 20:1–14
101. Moghtaderi H, Sepehri H, Delphi L, Attari F (2018) Gallic acid and curcumin induce cytotoxicity and apoptosis in human breast cancer cell MDA-MB-231. Bioimpacts 8:185
102. Wang R, Ma L, Weng D, Yao J, Liu X, Jin F (2016) Gallic acid induces apoptosis and enhances the anticancer effects of cisplatin in human small cell lung cancer H446 cell line via the ROS-dependent mitochondrial apoptotic pathway. Oncol Rep 35:3075–3083
103. Bataller R, Brenner DA (2005) Liver fibrosis. J Clin Invest 115:209–218
104. Paik Y-H, Schwabe RF, Bataller R, Russo MP, Jobin C, Brenner DA (2003) Toll-like receptor 4 mediates inflammatory signaling by bacterial lipopolysaccharide in human hepatic stellate cells. Hepatology 37:1043–1055
105. Gutiérrez-Venegas G, Contreras-Sánchez A, Ventura-Arroyo JA (2014) Anti-inflammatory activity of fisetin in human gingival fibroblasts treated with lipopolysaccharide. J Asian Nat Prod Res 16:1009–1017
106. Vittal R, Fisher A, Gu H, Mickler EA, Panitch A, Lander C, Cummings OW, Sandusky GE, Wilkes DS (2013) Peptide-mediated inhibition of mitogen-activated protein kinase–activated protein kinase–2 ameliorates bleomycin-induced pulmonary fibrosis. Am J Respir Cell Mol Biol 49:47–57
107. Liang J, Liu N, Liu X, Mena JM, Xie T, Geng Y, Huan C, Zhang Y, Taghavifar F, Huang G et al (2019) Mitogen-activated protein kinase–activated protein kinase 2 inhibition attenuates fibroblast invasion and severe lung fibrosis. Am J Respir Cell Mol Biol 60:41–48
108. Jin Y-K, Li X-H, Wang W, Liu J, Zhang W, Fang Y-S, Zhang Z-F, Dai H-P, Ning W, Wang C (2018) Follistatin-like 1 promotes bleomycin-induced pulmonary fibrosis through the transforming growth factor beta 1/mitogen-activated protein kinase signaling pathway. Chin Med J (Engl) 131:1917–1925
109. Chen H-M, Wu Y-C, Chia Y-C, Chang F-R, Hsu H-K, Hsieh Y-C, Chen C-C, Yuan S-S (2009) Gallic acid, a major component of Toona sinensis leaf extracts, contains a ROS-mediated anti-cancer activity in human prostate cancer cells. Cancer Lett 286:161–171
110. Abd-Elghany AA, Mohamad EA (2020) Ex-vivo transdermal delivery of Annona squamosa entrapped in niosomes by electroporation. J Radiat Res Appl Sci 13:164–173

Publisher's Note